JOURNAL OF NANO- AND ELECTRONIC PHYSICS
Vol. **8** No 2, 02011(5pp) (2016)

ЖУРНАЛ НАНО- ТА ЕЛЕКТРОННОЇ ФІЗИКИ
Том **8** № 2, 02011(5cc) (2016)

Ferromagnetism in Mn-doped Chalcopyrite $AlGaP_2$ Semiconductor

Byung-Sub Kang[1,*], Kie-Moon Song[1,†], Haeng-Ki Lee[2]

[1] *Nanotechnology Research Center, Nanoscience & Mechanical Engineering, Konkuk University, Chungju, 27478, South Korea*
[2] *Department of Radiotechnology, Suseong College, Daegu, 42078, South Korea*

(Received 03 March 2016; published online 21 June 2016)

The electronic property and the magnetism of $AlGaMnP_2$ compound by 3.125 %, 6.25 %, and 9.375 % Mn concentrations were investigated using the first-principles calculations. The Mn-doped $AlGaP_2$ chalcopyrite with or without defect of Al, Ga, or P atom yields a strong half-metallic ground state. The ferromagnetic state is the most energetically favorable one. The spin-polarization of Mn dopant is stable with a magnetic moment close to $4\mu_B$ due to intra-atomic exchange coupling. The states of host Al, Ga, or P atoms at the Fermi level are mainly a P-3*p* character, which mediates a strong interaction between the Mn-3*d* and P-3*p* states. The ferromagnetic state with high magnetic moment is originated from the hybridized P(3*p*)-Mn(3*d*)-P(3*p*) interaction formed through the *p-d* coupling without the defects. It is noted that the ferromagnetism arises from two distinguishing characteristics by polarons and by holes-mediated exchange-coupling.

Keywords: Chalcopyrite semiconductor, Band-structure, Ferromagnetism, First-principles.

DOI: 10.21272/jnep.8(2).02011 PACS numbers: 71.15.Ap, 71.55.Gs

1. INTRODUCTION

Diluted magnetic semiconductors (DMSs) have paid much attention because the *s* and *p* electrons of the nonmagnetic materials and the spin from the magnetic dopant can be employed in spintronic devices [1-5]. The spin-polarization in the semiconductor has tended to disappear quickly by spin-flip scattering, when the charges of ferromagnetic (FM) matters are implanted as spin injectors. Until now, the opportunities of DMS's devices have been limited because the low solubility of magnetic ions in non-magnetic matters. Thus it is a great worth to handle the FM semiconductor because the difficulty in the spin-injection to make DMSs at room temperature.

It has been reported that the Mn-doped $ZnSnAs_2$ [6] and $ZnGeP_2$ [7] shows the ferromagnetism at 320 and 312 K, respectively. Newly synthesized a $MnGeP_2$ ternary compound has been reported as a semiconductor, whose crystal structure is chalcopyrite [8]. It has been reported that a $MnGeP_2$ exhibits ferromagnetism with $T_c = 320$ K and a magnetic moment per Mn at 5 K of 2.58 μ_B, and an indirect energy gap of 0.24 eV. In the working for Ion implantation of Cr or Mn at concentrations of 1-5 at. % in $Al_xGa_{1-x}P$ ($x = 0.24$, 0.38), the ferromagnetism above 100 K for Cr and 300 K for Mn in AlGaP has been reported [9, 10]. The Mn rather than Cr dopant appears to be a more promising a high temperature ferromagnetism of AlGaP.

AlP is unstable in air and oxidizers rapidly. However, ternary AlGaP material is used in device structure, we see it can enhance the Curie temperature above while maintaining material stability. Other recent experiments for Mn-doped GaP show the FM ordering above 300 K [11-13]. The Curie temperature is largely affected by a type in the matter and the density of carrier. The *p*-type shows much higher than that of undoped or *n*-type matters. Accordingly, it can find that the Curie temperature increases for the concentration of Mn dopant. In this paper, we had studied by using *ab-initio* calculations for the electronic properties and magnetic characteristics of (Al,Mn)-codoped to fabricate GaP-based DMS. In the system of AlGaP; Mn, we had observed FM ordering with high magnetic moment (3.7~4.2μ_B/Mn). We had predicted that AlGaP ternary compound can has a character of chalcopyrite semiconductor with a direct band gap.

2. COMPUTATIONAL DETAILS

This work was carried out using a self-consistent full-potential linear muffin-tin orbital (LMTO) method [14] based on spin density functional theory within the generalized gradient approximation (GGA). We used the exchange-correlation functional of Perdew-Burke-Ernzerhof scheme [15]. The radii of muffin-tin (MT) sphere for Mn (or Al, Ga) and P were chosen to be 2.4 and 1.9 a.u., respectively. The LMTO basis set and charge density in each MT sphere were expanded with real spherical harmonics up to $l = 6$, where l is the angular momentum defined inside each MT sphere. The LMTO basis functions for Mn and Ga atoms within the valence-energy were chosen as 4*s* and 3*d*, and 4*s*, 4*p*, and 3*d*, respectively. The electron wave function was expanded in plane wave with a cut-off energy of 159.12 eV, 232.56 eV, and 340.0 eV for the Mn-4*s* (or Al-3*s*), Mn-4*p* (or Al-3*p*), and Mn-3*d*, respectively. The relativistic effect for the valence electrons was taken into account by the scalar-relativistic approximation. The MT approximation was employed in order to describe the atomic potential, the effects of spin-orbital coupling of valence electrons were not included. The linear tetrahedron method [14] over a gamma-centered $4 \times 4 \times 4$ mesh in the Brillouin zone was used. The $4 \times 4 \times 4$ mesh is corresponding to 64 *k*-points. Using these *k*-points insured that the total energies and the

* kangbs@kku.ac.kr
† kmsong@kku.ac.kr

magnetic moments were converged on a better 10 meV/cell and 0.01 μ_B/atom, respectively. Broyden and linear mixing strategies for the input and the output charge-density were used to accelerate convergence of spin and charge densities [14]. The electronic structure and magnetic properties on the (Al,Mn)-codoped GaP semiconductor had been performed. We had investigated for three Mn concentrations of 3.125 %, 6.25 %, and 9.375 %.

3. RESULTS AND DISCUSSION

A. *Structural properties*

The atomic structure of Al-doped GaP was considered as the tetrahedrally-coordinated zinc-blende materials. The chalcopyrite is a class of semiconductor confirmed as a promising material to fabricate nonlinear optical devices. The III-III-V_2 alloy crystallizes in a form of $AlGaP_2$ chalcopyrite structure. The tetrahedral chalcopyrite structure was displayed in the Fig. 1. First, we performed the atomic geometry and positions of the structures are fully relaxed until the force between atoms is less than 1.0 mRy/Bohr. For the AlP, GaP, and pure $AlGaP_2$ systems, we considered the atomic relaxations for the positions of the structures. However, the distortions of near host atoms by substituting Mn dopant in the $AlGaP_2$ bulk were neglected. For the AlP, GaP, and $AlGaP_2$ systems, the obtained lattice parameters from first-principles calculations are a = 5.726 Å and c = 11.452 Å for GaP; a = 5.648 Å and c = 11.296 Å for AlP. For $AlGaP_2$, they are a = 5.685 Å, c = 11.222 Å, and c/a = 1.974. For the GaP and AlP systems, the total-energy minimization of the supercell with keeping a c/a = 2.0 was performed. For the $AlGaP_2$ system, we considered the structural relaxation for each of a and c-axis. The calculated parameters for GaP and AlP can be compared with that of the zinc-blende structure. The experimental values are a = 5.451 Å and 5.450 Å for GaP [16, 17] and AlP [16], respectively. These chalcopyrite structures for GaP, $AlGaP_2$, and AlP exhibit the semiconducting character with energy gaps of 1.679 eV, 1.241 eV, and 0.276 eV, respectively. For the ternary alloys, the variation of the lattice parameter for each crystalline and the energy gap with compositions were shown in Fig. 2. It can be seen a downward bowing of the lattice parameter as increases Al concentration in the $Al_xGa_{1-x}P_2$ system (x = 0.0, 0.25, 0.75, and 1.0). While for the calculated band-gap, it increases from 0.276 eV to 1.679 eV. The calculated result of bandgap is smaller than that of the experiment [18]. It is general trend that the results by using the GGA are less than half of that of the experiment. Maybe it can be

Table 1 – Migration energies of Mn into the interstitial or on the defect sites with Mn concentration of 3.125 % and with the defect site of Al, Ga, or P atom. $E^{m}_{int,\,Mn}$ and $E^{m}_{d,\,Mn}$ denotes the systems of Mn-doped on the interstitial site (see Fig. 1) and on the defect site of Al, Ga, or P atom, respectively

Defect elements	$E^{m}_{int,\,Mn}$ (eV)	Magnetic moment (μ_B/Mn)	$E^{m}_{d,\,Mn}$ (eV)	Magnetic moment (μ_B/Mn)
Al	– 3.359	3.65	+ 0.455	3.79
Ga	– 2.660	3.64	– 0.338	3.87
P	– 5.229	3.18	+ 0.914	2.75

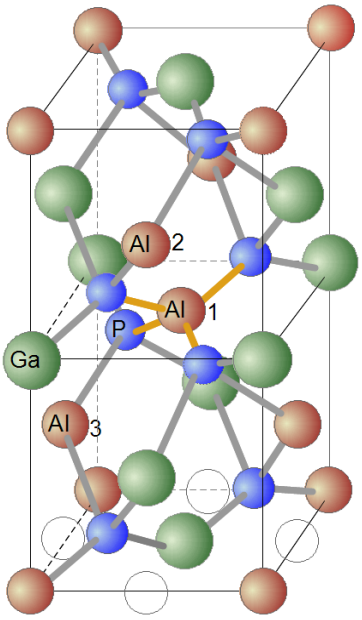

Fig. 1 – Supercell of chalcopyrite $AlGaP_2$. Open-circles represent interstitial sites in a layer. The numbers of 1, 2, or 3 denote the substitutional sites by Mn atoms

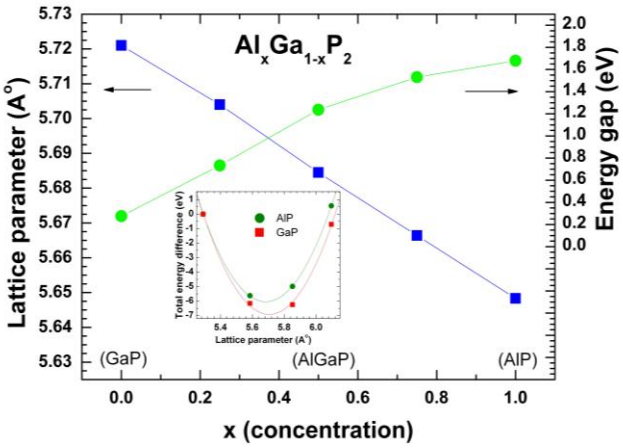

Fig.2 – Optimal lattice constants, a, and calculated band-gap for $Al_xGa_{1-x}P_2$ alloys. Total-energy differences as a function of lattice parameter for the GaP and AlP structures are shown in the inset

obtained the result that the calculated value in the LDA + U [19] is slightly larger than that in the GGA.

The (Al, Mn)GaP_2 and Al(Ga, Mn)P_2 corresponds to the case of Ga-rich and Al-rich systems, respectively. We observed that the Al(Ga, Mn)P_2 is the lowest energetically favorable system with or without a vacancy of Al, Ga, or P atom. The Al(Ga, Mn)P_2 is more energetically favorable than the (Al, Mn)GaP_2. For the defect systems, it can be seen in the Table 1. In the case of without a vacancy, the difference in the substitution energies between the (Al, Mn)GaP_2 and Al(Ga, Mn)P_2 is very small. Their energy are – 346.5 meV/Mn and - 282.2 meV/Mn for Al(Ga, Mn)P_2 and (Al, Mn)GaP_2, respectively. In the case of with a Ga vacancy, the migration energy of Mn into a defect site is the lowest by - 0.338 eV as compared to that of other system as seen in Table 1. The migration energy of Mn atom into the interstitial or the defect sites was defined as

$$E^{m}_{int/d\ Mn} = E(AlGaP_2;V(Al/Ga/P);Mn) - E(AlGaP_2) - n_1\mu_{Mn} + n_2\mu_{Al} + n_3\mu_{Ga} + n_4\mu_P$$

Here, $E(AlGaP_2;V(Al/Ga/P);Mn)$ and $E(AlGaP_2)$ are the total energies of Mn-doped $AlGaP_2$ with a vacancy of Al, Ga, or P and the pure $AlGaP_2$ systems for the supercell of the same size, respectively. The integer n_1, n_2, n_3, and n_4 are the number of doped Mn atoms on the Al, Ga, and P sites. The μ_{Mn}, μ_{Al}, μ_{Ga}, and μ_P are the atomic chemical potentials of Mn, Al, Ga, and P. The chemical potentials will be depended on the experimental conditions. The relationship of $\mu_{Al} + \mu_{Ga} + 2\mu_P = \mu_{AlGaP2}$ is formulated in thermal equilibrium of $AlGaP_2$. The μ_{Mn} will be determined by the equilibrium of bulk MnP, which has the FM phase with a Neel's temperature of 291 K [20]. $\mu_{Al} = E(AlP) - E(P)$ and $\mu_{Ga} = E(GaP) - E(P)$. For Al-rich system, $\mu_{Mn} = E(MnP) - E(AlP) + E(Al)$ and $\mu_P = E(AlP) - E(Al)$; and for Ga-rich system, $\mu_{Mn} = E(MnP) - E(GaP) + E(Ga)$ and $\mu_P = E(GaP) - E(Ga)$.

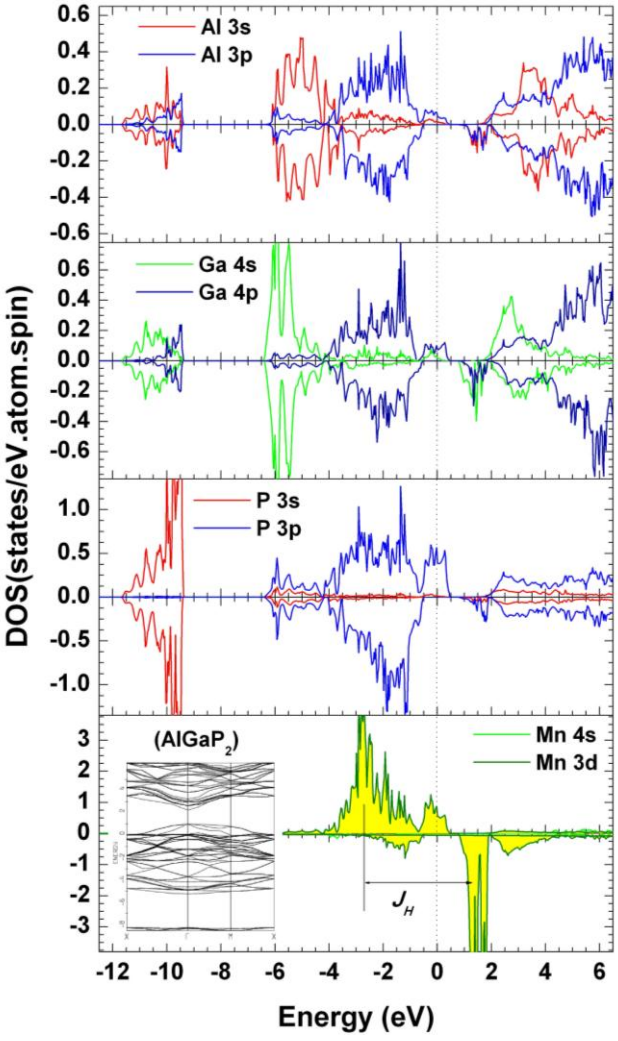

Fig. 3 – DOS for Al, Ga, P, and Mn sites of 6.25 % Mn-doped $AlGaP_2$ within FM state. The dotted line at zero presents the E_F. Energy-band along symmetry direction of $AlGaP_2$ is shown in the inset, indicating semiconducting character with direct bandgap

B. Electronic properties

Fig. 3 illustrates the partial density of states (DOS) for $Al_{1-y}Mn_yGaP_2$ at $y = 0.0625$. We could find the perturbation of valence state by Mn atom in the $AlGaP_2$. The minority-band shifts downward by about 0.5 eV in comparison with un-doped $AlGaP_2$. While the majority-band shifts upward by about 0.5 eV. It is formed a localized state just at the Fermi energy (E_F). We could find that the majority band on the E_F is mainly composed of Al-3*p* and Ga-4*p*, and P-3*p* states. The majority Mn-3*d* state is occupied at the low-energy region below the E_F, while the minority Mn-3*d* state contributes to the high energy region above the E_F. These majority *p* states make a result of strong hybridization between the P-3*p* (or Al-3*p*, or Ga-4*p*) and Mn-3*d* (t_2, d_{xy}) bands, or Mn-3d (e, d_{x2-y2}) bands. J_H is corresponds to the bandwidth between Mn-3*d* majority and minority states (see Fig. 3). The P-3*s* state is localized below $E_F - 10.5$ eV. The partially filled Mn *e*-band lies on the E_F (mainly majority states), while the t_2-band goes down in the valence band by $E_F - 2.5$ eV. The electron overlap indicates that there is the hybridizations between the Mn-*3d* and 3*p* (or 4*p*) electrons of P, Al, or Ga atom. Especially, a strong interaction between the Mn-3*d* and P-3*p* electrons is induced because an accumulation of carrier between these states just on the E_F. Hence the partially filled P-3*p* band contributes to the ferromagnetism with high magnetic moment. These configurations provide a clue to explicate the characteristics of holes-mediated ferromagnetism in the Mn-doped $AlGaP_2$ DMS. The ferromagnetism is stable by intra-atomic exchange interaction (Hund's coupling).

The Mn dopant orders ferromagnetically in $AlGaP_2$. The FM state is energetically stable as compared with the non-magnetic or antiferromagnetic (AFM) state. The total-energy difference between the FM and AFM states is – 99.7 meV in the Mn concentration of 6.25 %. For $Al_{1-y}Mn_yGaP_2$ for $y = 0.0625$ without a vacancy, the nearest neighboring four surrounding P atoms formed the MnP_4 tetrahedron are aligned positively with magnetic moments of $0.05\mu_B$ per P atom. While for the nearest neighboring Al or Ga atoms, it is aligned negatively with magnetic moment of ~ $-0.02\mu_B$ per Al or Ga atom. The substituted Mn atom has a high magnetic moment with $3.84\mu_B$ per Mn atom. The magnetic property of Mn atom is maintained to the ferromagnetism with a high-spin state as increasing up to the concentration of 9.375 % Mn. The magnetic moment is nearly constant. For the system with the vacancy of 3.125 % Al, Ga, or P, the magnetic moment of the nearest neighboring P atom to the vacancy is aligned negatively, while for the nearest neighboring Al, Ga, or Mn atoms, it is aligned positively. The Mn magnetic moment is 3.7~4.2μ_B per Mn atom. The Mn-doped $AlGaP_2$ with or without a vacancy is retained a strong half-metallic character. However, it is disappeared the half-metallic property in the case of Mn migration into the interstitial site. These results were listed Fig. 4, Fig. 5, and Table 2.

The origin of ferromagnetism of the half-metallic DMS with the defects can be explicated by bound magnetic polaron (BMP) [20]. This is that the exchange

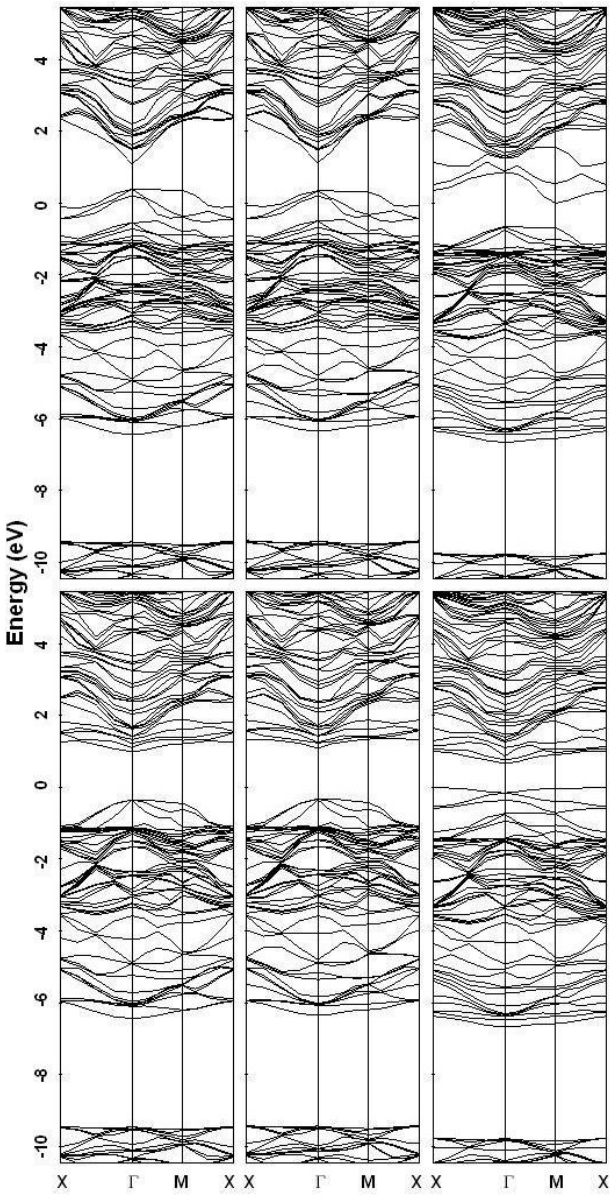

Fig. 4 – Band structures for 3.125 % Mn-doped $AlGaP_2$ on the defect site of Al (left), Ga (mid), and P (right) in the FM state. Up-three-panel indicates the majority-spin state. Down-three-panel indicates the spin-down state

interaction between the localized carriers trapped by vacancy and the spin-polarization of neighboring Mn^{2+} ions forms a BMP. A large BMP through the supercell gives rise to the ferromagnetism. The BMP is stable under a strong localization of carriers. For the half-metallic DMS without the defects, the FM state arises from the holes-mediated characteristics. The states of Ga-3*d* electrons is very little at the near the E_F. It is localized below a – 12 eV in the core region. So, the *d*-*d* interaction between the Ga and Mn atoms is very weak. The substituted system of Al by Mn atom and the system of Mn migration show the half-metallicity by downward shift of Al, Ga, and P minority bands. The Mn-P bond is a covalent due to the hybridizations between the Mn-3*d* and P-3*p* electrons. The direct *d*-*d* interaction between Mn atoms may be small because the variance of magnetic moment for the Mn concentration is nearly constant. Thus the ferromagnetism of Mn dopant maybe imply a direct exchange mechanism by the P site.

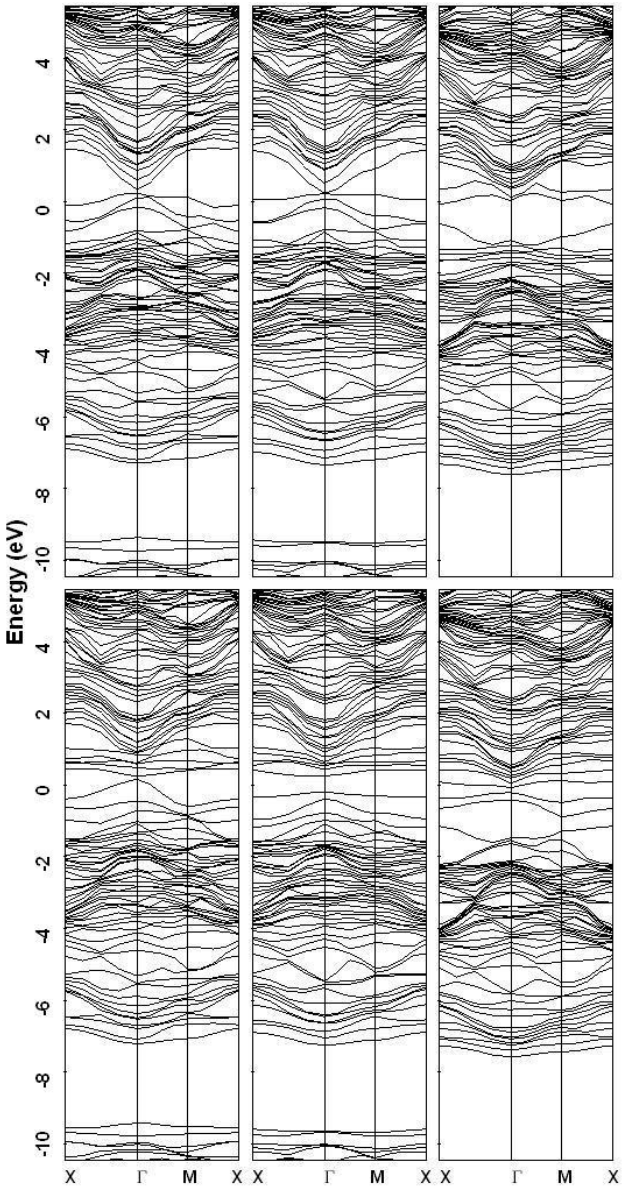

Fig.5 – Band structures for 3.125 % Mn-doped $AlGaP_2$ with the defect into the interstitial site in the FM state. Up-three-panel indicates the spin-up state. Down-three-panel indicates the spin-down state

4. CONCLUSION

We had studied the magnetism and electronic properties for Mn dopant in the chalcopyrite $AlGaP_2$ semiconductor by using the full-potential LMTO method. The systems of $Al_xGa_{1-x}P_2$ (x = 0.0, 0.25, 0.75, and 1.0) and Mn-doped $AlGaP_2$ with or without the defects by Mn concentration of 3.125, 6.25, and 9.375 had been investigated. The $AlGaP_2$ compound is a *p*-type semiconductor with a band gap of 1.24 eV. The FM state is the most stable with increasing of Mn-doping concentration. We had observed that these systems with or without the defects exhibit the half-metallic FM state. The FM ordering of Mn dopant and four neighboring P

Table 2 – Charge transfer from Mn site and charge transfer into a vacancy site within the defect site of 3.125 %. Magnetic moments of the nearest neighboring Mn, Al, Ga, and P from the defect site with respect to the Mn concentration of 3.125, 6.25, and 9.375 %

Defect elements	Mn Concentrations (%)	Charge transfer of Mn site	Charge transfer to defect site	Magnetic moments (μ_B)			
				Mn	Al	Ga	P
Al	3.125	1.051e	0.212e	3.65	+ 0.01	+ 0.01	– 0.27
	6.250	1.072e	0.210e	3.73	+ 0.01	+ 0.01	– 0.11
Ga	3.125	1.064e	0.208e	3.50	+ 0.00	+ 0.01	– 0.23
	6.250	1.067e	0.207e	3.65	+ 0.01	+ 0.02	– 0.33
P	3.125	1.189e	0.280e	4.28	+ 0.01	+ 0.02	– 0.01
	6.250	1.192e	0.256e	4.22	+ 0.02	+ 0.02	– 0.01
	9.375	1.188e	0.239e	4.15	+ 0.02	+ 0.03	– 0.03

atoms are produced by strong *p-d* hybridization. We had noted that a high magnetic moment of Mn is maintained by the hybridized P(3*p*)-Mn(3*d*)-P(3*p*) interaction in the case of without a vacancy. In conclusion, there are two distinguishing characteristics by polarons in the case of with a vacancy and by holes-mediated exchange coupling in the case of without a vacancy.

AKNOWLEDGEMENTS

This work was supported by Konkuk University (Dept. of Nano science and Mechanical engineering) in 2016.

REFERENCES

1. R.Y. Umetsu, H. Ishikawa, K. Kobayashi, A. Fujita, K. Ishida, R. Kainuma, *Scripta Mater.* **65**, 41 (2011).
2. C. Liu, F. Yun, H. Morkoç, *J. Mater. Sci.: Mater. Electron.* **16**, 555 (2005).
3. S.J. Pearton, C.R. Abernathy, D.P. Norton, A.F. Hebard, Y.D. Park, L.A. Boatner, J.D. Budai, *Mater. Sci. Eng. R* **40**, 137 (2003).
4. J.M.D. Coey, *Curr. Opin. Solid St. M.* **10**, 83 (2006).
5. A. Hirohata, M. Kikuchi, N. Tezuka, K. Inomata, J.S. Claydon, Y.B. Xu, G. van der Laan, *Curr. Opin. Solid St. M.* **10**, 93 (2006).
6. S. Choi, G.-B. Cha, S.C. Hong, S. Cho, Y. Kim, J.B. Ketterson, S.-Y. Jeong, G.-C. Yi, *Solid State Commun.* **122**, 165 (2002).
7. Sunglae Cho, Sungyoul Choi, Gi-beom Cha, Soon Cheol Hong, Yunki Kim, Yu-Jun Zhao, Arthur J. Freeman, John B. Ketterson, B.J. Kim, Y.C. Kim, Byung-Chun Choi, *Phys. Rev. Lett.* **88**, 257203 (2002).
8. Sunglae Cho, Sungyoul Choi, Gi-Beom Cha, Soon Cheol Hong, Yunki Kim, Arthur J Freeman, John B. Ketterson, Yongsup Park, Hyun-Min Park, *Solid State Commun.* **129**, 609 (2004).
9. M.E. Overberg, G.T. Thaler, R.M. Frazier, C.R. Abernathy, S.J. Pearton, R. Rairigh, J. Kelly, N.A. Theodoropoulou, A.F. Hebard, R.G. Wilson, J.M. Zavada, *J. Appl. Phys.* **93**, 7861 (2003).
10. M.E. Overberg, G.T. Thaler, R.M. Frazier, C.R. Abernathy, S.J. Pearton, R. Rairigh, J. Kelly, N.A. Theodoropoulou, A.F. Hebard, R.G. Wilson, J.M. Zavada, *J. Vac. Sci. Technol. B* **21** No 5, 2093 (2003).
11. T. Dietl, *J. Appl. Phys.* **89**, 7437 (2^01).
12. N. Theodoropoulou, A.F. Hebard, M.E. Overberg, C.R. Abernathy, S.J. Pearton, S.N.G. Cha, R.G. Wilson, *Phys. Rev. Lett.* **89**, 107203 (2002).
13. M.E. Overberg, B.P. Gila, G.T. Thaler, C.R. Abernathy, S.J. Pearton, N.A. Theodoropoulou, K.T. McCurthy, S.B. Arnason, A.F. Hebard, S.N.G. Cha, R.G. Wilson, J.M. Zavada, Y.D. Park, *J. Vac. Sci. Technol. B* **20**, 969 (2002).
14. S.Yu. Savrasov, *Phys. Rev. B* **54**, 16470 (1996).
15. J.P. Perdew, K. Burke, M. Ernzerhof, *Phys. Rev. Lett.* **77**, 3865 (1996).
16. C. Kittel, *Introduction to Solid State Physics Seventh ed.* (John Wiley & Sons: 1996).
17. Nadir Bouarissa, *Mater. Chem. Phys.* **124**, 336 (2010).
18. S.J. Pearton, C.R. Abernathy, D.P. Norton, A.F. Hebard, Y.D. Park, L.A. Boatner, J.D. Budai, *Mater. Sci. Eng. R* **40**, 137 (2003).
19. J.H. Park, S.K. Kwon, B.I. Min, *Physica B* **281-282**, 703 (2000).
20. J.M.D. Coey, M. Venkatesan, C.B. Fitzgerald, *Nat. Mater.* **4**, 173 (2005).